The Journal of Immunology

Mitochondrial Dysfunction Increases Allergic Airway Inflammation

Leopoldo Aguilera-Aguirre, Attila Bacsi, Alfredo Saavedra-Molina, Alexander Kurosky, Sanjiv Sur and Istvan Boldogh

J Immunol 2009; 183:5379-5387; Prepublished online 28 September 2009;
doi: 10.4049/jimmunol.0900228
http://www.jimmunol.org/content/183/8/5379

The Journal of Immunology is published twice each month by
The American Association of Immunologists, Inc.,
1451 Rockville Pike, Suite 650, Rockville, MD 20852

Print ISSN: 0022-1767 Online ISSN: 1550-6606.

Mitochondrial Dysfunction Increases Allergic Airway Inflammation[1]

Leopoldo Aguilera-Aguirre,*§ Attila Bacsi,*¶ Alfredo Saavedra-Molina,§ Alexander Kurosky,† Sanjiv Sur,‡ and Istvan Boldogh*[2]

The prevalence of allergies and asthma among the world's population has been steadily increasing due to environmental factors. It has been described that exposure to ozone, diesel exhaust particles, or tobacco smoke exacerbates allergic inflammation in the lungs. These environmental oxidants increase the levels of cellular reactive oxygen species (ROS) and induce mitochondrial dysfunction in the airway epithelium. In this study, we investigated the involvement of preexisting mitochondrial dysfunction in the exacerbation of allergic airway inflammation. After cellular oxidative insult induced by ragweed pollen extract (RWE) exposure, we have identified nine oxidatively damaged mitochondrial respiratory chain-complex and associated proteins. Out of these, the ubiquinol-cytochrome *c* reductase core II protein (UQCRC2) was found to be implicated in mitochondrial ROS generation from respiratory complex III. Mitochondrial dysfunction induced by deficiency of UQCRC2 in airway epithelium of sensitized BALB/c mice prior the RWE challenge increased the Ag-induced accumulation of eosinophils, mucin levels in the airways, and bronchial hyperresponsiveness. Deficiency of UQCRC1, another oxidative damage-sensitive complex III protein, did not significantly alter cellular ROS levels or the intensity of RWE-induced airway inflammation. These observations suggest that preexisting mitochondrial dysfunction induced by oxidant environmental pollutants is responsible for the severe symptoms in allergic airway inflammation. These data also imply that mitochondrial defects could be risk factors and may be responsible for severe allergic disorders in atopic individuals. *The Journal of Immunology,* **2009, 183: 5379–5387.**

Prevalence of allergic airway inflammation and asthma has become an increasing problem in the United States and other developed countries. There are indications that complex interactions between genetic and environmental factors have a role in the development of these diseases (1). Environmental factors, including ozone, diesel exhaust particles, and tobacco smoke, as well as respiratory virus infections, which are known to increase the production of reactive oxygen species (ROS)[3] in the airway epithelium, exacerbate allergic inflammation in asthma (2). Excessive levels of ROS can trigger signaling cascades and/or cause oxidative damage to cellular and mitochondrial macromolecules, resulting in mitochondrial dysfunction (3, 4). It has also been shown that environmental oxidants induce oxidative damage to mitochondria in the airways (5–7). Pollen grains and subpollen particles have intrinsic NADPH oxidases and upon hydration they produce ROS (8, 9). ROS generated by these pollen enzymes induce oxidative stress in the airway epithelium, resulting in increased inflammatory chemokine and cytokine production and exacerbation of airway inflammation (8, 10). Repeated pollen challenges within a limited time period increase the allergic responses to Ags (11, 12). These observations raise the possibility of a sustained cellular injury in the airway, which makes the immune machinery more responsive to a subsequent antigenic stimulus.

The catalytic antioxidant AEOL 10113, which mimics the effect of superoxide dismutase (13), is able to enter mitochondria and protect the electron transport chain from oxidative damage (14). Importantly, intratracheal administration of AEOL 10113 significantly decreased allergen-induced airway hyperreactivity to methacholine and the severity of airway inflammation, as evidenced by the reduced numbers of inflammatory cells in bronchoalveolar lavage fluid (BALF) (15). These observations are consistent with mitochondrial dysfunction and ultrastructural changes observed as consequences of airway inflammation in a similar model of experimental allergic asthma (16). The exclusively maternal transmission of mitochondria in humans (17) and the epidemiological link between maternal history of asthma and a greater risk for atopy in descendants (18, 19) suggest an involvement of mitochondria in allergy susceptibility. Indeed, there is a strong association between mitochondrial genomic sequence variation and total serum IgE levels and atopy (20).

*Department of Microbiology and Immunology, †Department of Biochemistry and Molecular Biology, and ‡Department of Internal Medicine, University of Texas Medical Branch at Galveston, Galveston, TX 77555; §Instituto de Investigaciones Químico-Biológicas, Universidad Michoacana de San Nicolás de Hidalgo, Morelia, Michoacán, México; and ¶Institute of Immunology, Medical and Health Science Center, Faculty of Medicine, University of Debrecen, Debrecen, Hungary

Received for publication January 22, 2009. Accepted for publication August 16, 2009.

The costs of publication of this article were defrayed in part by the payment of page charges. This article must therefore be hereby marked *advertisement* in accordance with 18 U.S.C. Section 1734 solely to indicate this fact.

[1] This work was supported by National Institute of Allergy and Infectious Diseases Grant P01 AI062885-01 (to I.B. and S.S.), National Institutes of Health Grant HL071163 (to S.S. and I.B.), National Institutes of Health, National Heart, Lung, and Blood Institute Proteomics Initiative NO1HV-28184 (to A.K.), National Institute on Environmental Health Sciences Center Grant EOS 006677 (to I.B. and A.K.), and the Hungarian Scientific Research Fund 73347 (to A.B.).

[2] Address correspondence and reprint requests to Dr. Istvan Boldogh, Department of Microbiology and Immunology, University of Texas Medical Branch at Galveston, 301 University Boulevard, Galveston, TX 77555. E-mail: sboldogh@utmb.edu

[3] Abbreviations used in this paper: ROS, reactive oxygen species; ASO, antisense oligonucleotides; BALF, bronchoalveolar lavage fluid; Cox IIb, cytochrome *c* oxidase subunit IIb; DAPI, 4,6′-diamidino-2-phenylindole; DCF, dichlorofluorescein; DNPH, 4-dinitrophenylhydrazine; DPI, diphenylene iodonium; H_2DCF-DA, 2′-7′-dihydrodichlorofluorescein diacetate; mtDNA, mitochondrial DNA; MRC, mitochondrial respiratory complex; NAC, *N*-acetyl-L-cysteine; NDUFS1, NADH dehydrogenase (ubiquinone) Fe-S protein 1; NDUFS2, NADH dehydrogenase (ubiquinone) Fe-S protein 2; 3-NPA, 3-nitropropionic acid; Penh, enhanced pause; RWE, ragweed pollen extract; UQCRC1, ubiquinol-cytochrome *c* reductase core protein I; UQCRC2, ubiquinol-cytochrome *c* reductase core protein II.

Whether exposure to pollen induces oxidative damage to mitochondria in airway epithelial cells, as well as the association between preexisting mitochondrial dysfunction and severe allergic inflammatory symptoms, has not been investigated. Herein we identified oxidatively damaged mitochondrial proteins after ragweed pollen extract (RWE) exposure, among which was a respiratory complex III protein, ubiquinol-cytochrome *c* reductase core protein II (UQCRC2). We show that deficiency of UQCRC2 results in increased ROS production in airway epithelial cells. Animals expressing lower levels of UQCRC2 in the airways have a significantly higher degree of RWE-induced airway inflammation and bronchial hyperresponsiveness compared with control mice challenged with RWE only. These results suggest that preexisting mitochondrial dysfunction intensifies Ag-driven allergic airway inflammation and it could be a risk factor for development of allergic disorders in susceptible individuals.

Materials and Methods

Cell cultures

Human alveolar epithelial cells (A549) and mouse lung adenoma cells (LA-4) were obtained from American Type Cell Collection and cultured in Ham's F-12 medium supplemented with 10% (A549) or 15% (LA-4) heat-inactivated FBS, L-glutamine (2 mM), penicillin (100 U/ml), and streptomycin (100 μg/ml) at 37°C in a humidified atmosphere with 95% air and 5% CO_2. Mitochondrial DNA (mtDNA)-depleted cells (ρ0) were developed as we had previously described (21). Briefly, A549 cell cultures were maintained in complete growth medium supplemented with 50 ng/ml ethidium bromide for >60 population doublings. Respiration-deficient cells became pyrimidine auxotrophs, and hence medium was supplemented with uridine (50 μg/ml) and sodium pyruvate (120 μg/ml) (22). Depletion of mtDNA was confirmed by Southern blot hybridization as previously described (23).

Measurement of intracellular ROS levels

Cells in suspension were loaded with 5 μM 2′,7′-dihydro-dichlorofluorescein diacetate (H_2DCF-DA) for 15 min at 37°C. After removing excess H_2DCF-DA, cells were treated with 100 μg/ml RWE and the changes in dichlorofluorescein (DCF) fluorescence were determined at different time points by flow cytometry (BD FACSCanto flow cytometer; BD Biosciences). Each datum point represents the mean fluorescence of 12,000 cells from three or more independent experiments. Alternatively, in parallel experiments, cells at 70% confluence were loaded with 50 μM H_2DCF-DA on 24-well plates (Costar). Changes in fluorescence intensity in mock-treated and RWE-treated cells were measured using an FLx800 microplate fluorescent reader (BioTek Instruments) at 488 nm excitation and 530 nm emission wavelengths.

Mitochondria isolation and purification

Mitochondria were isolated and purified as we have previously described (21, 24). Briefly, cell pellets were incubated in buffer A (220 mM mannitol, 70 mM sucrose, 2 mM MOPS, and 1 mM EGTA (pH 7.4)) containing protease inhibitor cocktail (Sigma-Aldrich, catalog no. P8340). Cell suspensions kept in an ice bath were sonicated with a Branson sonifier by four pulses of 20% power, and cell homogenates were centrifuged for 10 min at 4700 × *g*. Mitochondria were sedimented from supernatants by centrifugation at 7168 × *g*. Pellets were resuspended in buffer B (220 mM mannitol, 70 mM sucrose, 2 mM MOPS (pH 7.4)) and centrifuged at 9072 × *g*. Crude mitochondrial solutions were layered on discontinuous sucrose gradients (1.5, 1.0, and 0.5 M sucrose in 10 mM MOPS and 1 mM EDTA (pH 7.4)) (25) and ultracentrifuged for 1.5 h at 82,705 × *g* (SW28 rotor; Beckman Coulter). All centrifugation procedures were conducted at 4°C. The band containing mitochondria was removed and washed in 10× vol of buffer B. Mitochondrial pellets were resuspended in buffer B containing protease inhibitor cocktail (Sigma-Aldrich) and kept at −80°C.

Isolation of mitochondrial respiratory complexes

Mitochondrial respiratory complexes (MRCs) were isolated by blue native PAGE as previously described (26). Briefly, mitochondria (200 μg of protein) were solubilized in 50 mM imidazole-HCl, 750 mM 6-aminocaproic acid (pH 7.0), and dodecyl maltoside (at a detergent-protein weight ratio of 1:4) for 30 min at 4°C and centrifuged at 16,100 × *g*. The supernatant was supplemented with Coomassie brilliant blue G-250 (at a dye-protein weight ratio of 1:4) and 10% glycerol, and MRCs were electrophoresed in a 5–12% blue native PAGE (27). Mitochondrial respiratory complex bands were excised from the gel and incubated in a denaturing buffer (6% SDS, 150 mM 2-ME) and then placed on a 10% SDS-PAGE to separate individual proteins. To confirm the identity of respiratory complexes, a MS601 MitoProfile Human Total OXPHOS Complexes Detection kit (MitoSciences) was used according to the manufacturer's protocol.

Detection of oxidized proteins

Changes in oxidized protein levels were determined using an Oxyblot kit (Chemicon/Millipore) according to the manufacturer's recommendations. Briefly, proteins were derivatized with 4-dinitrophenylhydrazine (DNPH) for 15 min followed by incubation at room temperature with a neutralization buffer (Chemicon/Millipore). Derivatized proteins were electrophoresed on a 10% SDS-PAGE and blotted on Hybond polyvinylidene difluoride membranes (Amersham Biosciences). Blots were blocked with 5% nonfat dry milk dissolved in Dulbecco's PBS containing 0.05% Tween 20 (PBS-T) for 3 h and incubated with anti-DNP primary Ab (1/150) (Chemicon/Millipore) overnight at 4°C. In selected experiments, blots were incubated with primary Ab to 4-hydroxynonenal protein adducts (1/300) (Oxis International). In control experiments, blots were analyzed for components of the mitochondrial respiratory chain complexes using OXPHOS mAb cocktail (1/200) (MitoSciences). After three washes with PBS-T, membranes were incubated for 1 h at room temperature with HRP-conjugated secondary Abs (1/300) (Amersham Biosciences). Immunocomplexes were visualized by chemiluminescence using the ECL kit (Amersham Biosciences).

Protein identification

Protein bands were excised from Coomassie blue-stained SDS-PAGE gels, digested with trypsin, and subjected to mass spectrum analysis using a model 4800 MALDI-TOF/MS analyzer (Applied Biosystems). Proteins were identified using the Swiss-Prot database and the Mascot algorithm as we reported previously (28). Expected values were considered significant when $E \leq 0.01$ (29). MS analyses were conducted by the Biomolecular Resource Facility at University of Texas Medical Branch at Galveston.

Amplex Red assay

Release of H_2O_2 from isolated mitochondria was measured by Amplex Red (10-acetyl-3,7-dihydroxyphenoxazine; Molecular Probes) assay as we previously described (21). Briefly, mitochondria (100 μg/ml) were suspended in 50 μl (per well) reaction buffer and incubated with 0.25 U/ml Amplex Red and 1 U/ml HRP at 25°C for 30 min. The changes in fluorescence intensity were measured using a microplate reader (SpectraMass M2; Molecular Devices) at 530/590 nm. The addition of catalase (400 U/ml; Sigma-Aldrich), which catalyzes the decomposition of H_2O_2 to water and oxygen, decreased fluorescence signals by 90%. As a positive control, increasing concentrations of H_2O_2 (0–400 pmol) were used.

Mitochondrial quality was assessed by respiratory control ratio as previously described (30). Mitochondrial respiratory state 4 (ST4, resting state) was determined by oxygen consumption rate in the presence of respiratory substrates (5 mM glutamate/5 mM malate or 10 mM succinate/1 μM rotenone). Respiratory state 3 (ST3, active state) was determined by oxygen consumption rate in the presence of respiratory substrates plus ADP and Pi. Respiratory control ratio was calculated as the ratio of ST3/ST4. Mitochondrial suspensions showing respiratory control ratio values >2.5 were used for additional experiments.

Down-regulation of target genes by antisense oligonucleotides

Antisense oligonucleotides (ASO) were designed by siDESIGN Center online software (Dharmacon RNAi Technologies) using the sequence database of the National Center for Biotechnology Information. The phosphorothioate protected ASO were synthesized by Integrated DNA Technologies. Down-regulation of target gene expression was evaluated by real-time RT-PCR. Total RNA was isolated using an RNAqueous kit (Ambion). A template of cDNA was synthesized using SuperScript III First-Strand Synthesis SuperMix for quantitative RT-PCR (Invitrogen). Real-time PCR primers for UQCRC1 (ubiquinol-cytochrome *c* reductase core protein I; catalog no. PPM41408A) and UQCRC2 (catalog no. PPM24606A) (SABiosciences) were used to analyze expression levels of these genes. To analyze transfection efficiency, Texas Red-labeled ASO were transfected into LA-4 cells. Four hours later, cells were dried, fixed in acetone/methanol (1/1), and stained with 10 ng/ml 4,6′-diamidino-2-phenylindole (DAPI). Cells were mounted on microscope slides and analyzed using a Nikon Eclipse TE 200 fluorescent microscope coupled to a Photometrix CoolSNAP Fx CCD digital camera and MetaMorph software

(version 6.09; Universal Imaging). Down-regulation of target genes by ASO was calculated based on percentage of transfected cells and levels of PCR amplification. For down-regulation of UQCRC1 and UQCRC2, the following ASO were selected: UQCRC1 (3′-t*c*t*tgcaccagaaact*a*a*t) and UQCRC2 (3′-g*g*t*acgacgataacaa*c*g*t) (*, phosphorothioate).

Sensitization and challenge of animals

BALB/c mice were purchased from Harlan Sprague Dawley. All animal experiments were performed according to the National Institutes of Health Guide for Care and Use of Experimental Animals and approved by the University of Texas Medical Branch at Galveston Animal Care and Use Committee. Eight-week-old female mice were sensitized with RWE as previously described (8). Briefly, mice received two i.p. administrations (days 0 and 4) of endotoxin-free (150 μg per animal) RWE (lot 34868; Greer Laboratories mixed with alum adjuvant (Pierce Laboratories) at a ratio of 3:1. RWE-sensitized mice received intranasally 10 μg of antisense dissolved in 60 μl of PBS at 36, 24, and 12 h before RWE challenge. Control mice received the same volumes of PBS. On day 11, mice were challenged intranasally with RWE (100 μg dissolved in 60 μl of PBS).

Assessment of UQCRC1 and UQCRC2 expression in the lungs

Levels of UQCRC1 and UQCRC2 proteins were analyzed by fluorescent microscopy as we previously described (8). Briefly, lung sections were blocked for 30 min with rabbit nonimmune serum (1/100). After two washes with PBS-T, slides were incubated with primary Abs to UQCRC1 (1/200) (Santa Cruz Biotechnology) and UQCRC2 (1:200) (Novus Biologicals) as well as to cytochrome *c* oxidase subunit IIb (Cox IIb; Molecular Probes) for 60 min at 30°C. After two washes with PBS-T, cells were incubated with FITC-conjugated (Santa Cruz Biotechnology) or Texas Red-conjugated (Leinco Technologies) $F(ab')_2$ secondary Abs (1/200) for 60 min at 37°C. After a wash with PBS-T, cells were counterstained with 10 ng/ml DAPI and mounted using Dako mounting medium. The stained sections were photographed with a Photometrix CoolSNAP Fx CCD digital camera mounted on a Nikon Eclipse TE 200 fluorescent microscope. Five to six images from five different levels per lung (n = 3–4 animals/group) were obtained and fluorescence intensities corresponding to UQCRC1, UQCRC2, as well as Cox IIb expression were measured using MetaMorph software (version 6.09). The data are represented as fluorescence intensity/μm^2 in the peribronchial area.

Differential cell counts

Three days after RWE challenge, mice were euthanized and BALF samples were collected. Briefly, tracheae were cannulated and lung lavage was performed by two instillations of 0.7 ml of ice-cold PBS. The BALF samples were centrifuged (800 × g for 5 min at 4°C), and the resulting supernatants were stored at −80°C for further analysis. Total cell counts in BALF were determined from an aliquot of the cell suspension. Differential cell counts were performed on cytocentrifuge preparations (Shandon Cytospin 4 Cytocentrifuge; Thermo Scientific) stained with Wright-Giemsa in a blind fashion by two independent researchers counting 800 cells from each cytospin preparation.

Assessment of mucin levels

MUC5AC levels in BALF were assessed by ELISA as previously described (31). Briefly, 96-well plates were coated with serially diluted BALF in coating buffer (50 mM Na_2CO_3, 50 mM $NaHCO_3$) and then primary mouse anti-human MUC5AC Ab (1/16,000) (clone 45M1; Lab Vision) was added. Binding of primary Ab was detected by peroxidase-conjugated goat anti-mouse secondary Ab (1/5000) (Amersham Biosciences) and a peroxidase substrate, tetramethyl benzidine (eBioscience). Changes in absorbance were measured at 450 nm using a SpectraMax 190 ELISA plate reader (Molecular Devices). All incubations were done at 37°C.

Evaluation of allergic inflammation by histology

After bronchoalveolar lavage, the lungs were fixed with 10% paraformaldehyde, embedded in paraffin, sectioned to 5 μm, and stained with H&E. Perivascular and peribronchial inflammation were evaluated by a pathologist in a blinded fashion to obtain data for each lung. Mucin-producing cells were assessed by periodic acid-Schiff staining of formalin-fixed, paraffin-embedded lung sections. The stained sections were analyzed as above and representative fields were photographed with a Photometrix CoolSNAP Fx camera mounted on a Nikon Eclipse TE 200 UV microscope.

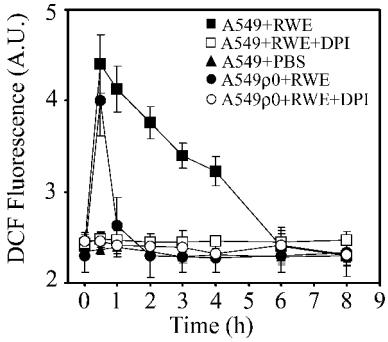

FIGURE 1. Exposure of cells with functional mitochondria results in a sustained increase in intracellular ROS levels. Airway epithelial cells (A549) and mitochondrial DNA depleted A549ρ0 cells were loaded with H_2DCF-DA and treated with 100 μg/ml RWE in the presence or absence of DPI, a NADPH oxidase inhibitor. Changes in intracellular DCF fluorescence were determined by flow cytometry. The datum points represent mean values of three independent experiments.

Airway hyperresponsiveness

Changes in pause of breathing (enhanced pause (Penh)) as an index of airway obstruction were measured by barometric whole-body plethysmography (Buxco Electronics) (32). Bronchial hyperreactivity was evaluated using methacholine challenges (33). Briefly, mice were placed in a Buxco chamber, allowed to acclimate for 5 min, and then exposed for 3 min to nebulized saline. Subsequently, mice were exposed to increasing concentrations (0, 6.25, 12.5, 25, and 50 mg/ml) of nebulized methacholine (Sigma-Aldrich) in saline. The median size of the aerosol droplets ranged between 1 and 4 μm (manufacturer's specification). Bronchopulmonary resistance was expressed as enhanced pause = [(expiratory time/relaxation time) − 1] × (peak expiratory flow/peak inspiratory flow). The flow signals and the respiratory parameters were calculated using the Biosystem XA program (Buxco Electronics).

Statistical analysis

Data are presented as means ± SEM. Mice were randomly grouped (group size, n = 4–6). All experiments were repeated three to five times. Statistical analysis was performed using Student's t test or ANOVA, followed by post hoc tests: Bonferroni's (samples with equal variances) and Dunnett's T3 (samples with unequal variances) with SPSS 14.0 software. Differences were considered to be statistically significant at $p < 0.05$.

Results

Exposure to pollen extract induces oxidative damage to mitochondrial respiratory chain proteins

Pollen grains or their extracts induce oxidative stress in cultured cells as well as in the airway epithelium and the conjunctiva of experimental animals (8, 34). Here we show that addition of RWE to human airway epithelial cells (A549), after an initial oxidative burst, resulted in a sustained increase in the intracellular ROS levels. At 6 h after RWE exposure, ROS levels decreased to basal values as shown in Fig. 1. On the other hand, in mtDNA-depleted cells (A549ρ*0*) the oxidative burst was transient and lasted for ~1 h (Fig. 1). Diphenylene iodonium (DPI; 100 μM), a NADPH oxidase inhibitor (35), abolished the changes in ROS levels in both A549 and A549ρ*0 cells* (Fig. 1). Taken together, these results suggested that RWE exposure causes oxidative modifications to cellular and mitochondrial proteins, resulting in sustained ROS generation from mitochondria.

Next, we isolated and purified mitochondria from RWE-treated and control cells. First, overall changes in modified protein levels were analyzed and, as shown in Fig. 2, a notable increase in carbonylated protein levels was observed in mitochondrial lysates from RWE-treated cells, but not from mock-treated cells. After that, the MRCs were isolated by blue native PAGE (Fig. 3*A*),

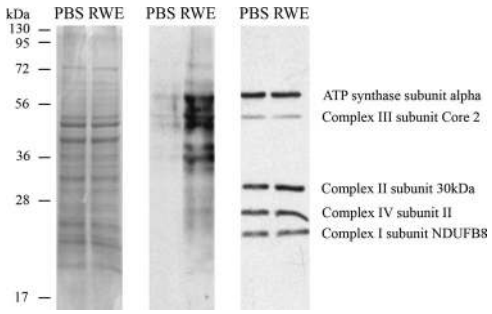

FIGURE 2. Treatment of epithelial cells with RWE increases the levels of carbonylated proteins in mitochondria. Mitochondria isolated from mock-treated and RWE-exposed (100 μg/ml) cells were purified (see *Materials and Methods*). Mitochondrial lysates were DNPH derivatized and subjected to SDS-PAGE (*left panel*). After blotting onto membrane, oxidatively damaged proteins were detected using DNP-specific Ab (*middle panel*). In parallel experiments, the relative levels of respiratory complex proteins in mitochondrial preparations were analyzed using OXPHOS mAb cocktail (*right panel*). Results are from a representative experiment from three repeats.

DNPH-derivatized, and their proteins were separated in 10% SDS-PAGE and damaged proteins were visualized by anti-DNP Ab. Levels of carbonylated proteins were increased in mitochondrial respiratory complexes and complex-associated proteins from RWE-treated cells compared with those from mock-treated ones (Fig. 3*B*). In complex I, anti-DNP Ab did not detect any DNPH-derivatized proteins from mock-treated cells, while it detected four carbonylated proteins from those treated with RWE (Fig. 3*B*, *right panel*, 1–4). In complex III, three protein bands appeared as a consequence of RWE treatment (Fig. 3*B*, *right panel*, 5–7). In complex IV, only quantitative differences in the levels of carbonylated proteins were observed (Fig. 3*B*). Due to RWE exposure, levels of carbonylated proteins further increased and an additional 31-kDa protein was oxidatively damaged in complex II (Fig. 3*B*, *right panel*, 14). Furthermore, we observed elevated levels of 4-hydroxynonenal protein adducts from RWE-treated cells (data not shown). Their patterns were similar; however, their abundances were less pronounced than those of carbonylated proteins.

MALDI-TOF/MS analysis of oxidatively damaged proteins identified NADH dehydrogenase (ubiquinone) Fe-S protein (NDUFS) 1 and NDUFS2, both of which are constituents of the catalytic core of complex I (Table I and Fig. 3). UQCRC1 and UQCRC2, core components of complex III, were also identified among the damaged proteins (Table I and Fig. 3). The localization of these proteins in the mitochondrial respiratory chain is illustrated in Fig. 10. We did not find carbonylated electron transport proteins in either complex II or IV. In all experiments, several accessory proteins, which co-migrated with the respiratory chain complexes during the blue native PAGE, were also damaged. These proteins include 75-kDa glucose-regulated protein (GRP75; associated with complex (C) III), heat shock protein (HSP) 70 (CI, CII, CIII, and CIV), HSP60 (CII and CIV), citrate synthase (CISY; CII), and voltage-dependent anion selective channel 1 (VDAC1; CII) (Table I and Fig. 3). All identified proteins are nuclear encoded, and the chromosomal localizations of their genes are shown in Table I.

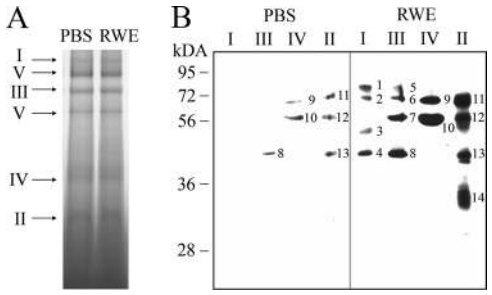

FIGURE 3. Detection and identification of carbonylated mitochondrial respiratory complex proteins. *A*, Mitochondria isolated from mock-treated and RWE-exposed (100 μg/ml) cells were purified. Equal amounts of mitochondrial lysates were loaded and MRCs were isolated on blue native PAGE. *B*, Complexes (I–IV) were excised from blue native gels and DNPH derivatized before separation on 10% SDS-PAGE. Carbonylated proteins were visualized using Ab to DNP. Oxidatively damaged proteins identified by MALDI-TOF/MS analysis are shown in Table I.

Pollen extract triggers ROS production from mitochondrial respiratory chain complex III

To analyze the functional consequences of oxidative damage to mitochondrial proteins, we determined the levels of ROS released from isolated mitochondria of RWE-treated and control cells. The primary mitochondrial reactive oxygen radical is the superoxide anion, which is rapidly converted to H_2O_2 by enzymatic or nonenzymatic pathways (36). Mitochondria isolated from RWE-treated cells produced a significantly higher amount of H_2O_2 than those from mock-treated cells (Fig. 4*A*). In control experiments, cells were exposed to heat-inactivated RWE (8) or they were treated with RWE in the presence of either DPI (100 μM) or antioxidant (*N*-acetyl-L-cysteine (NAC); 10 mM, 3-h pretreatment). The H_2O_2 productions of mitochondria from these cells were close to basal level. These data are in agreement with the notion that oxidative mitochondrial damage leads to elevated ROS production (37). Complex I (rotenone; 10 μM) or complex II (3-nitropropionic acid (3-NPA), 3 mM) inhibitors significantly decreased mitochondrial H_2O_2 production (Fig. 4*B*). The combined use of rotenone and 3-NPA decreased the H_2O_2 production nearly to the basal level (Fig. 4*B*), suggesting that electron flow from complex I and complex II is required for the increased ROS generation. Stigmatellin, which inhibits the Qo site of complex III at low concentration (0.06 μM) (38), abolished the RWE-induced mitochondrial H_2O_2 generation, while antimycin A (10 μM), an inhibitor of the electron transfer from cytochrome *b* to ubiquinone (21), further increased it, suggesting that complex III is the most likely source of the released ROS (Fig. 4*B*). The sites of action of these inhibitors are shown in Fig. 10. Taken together, these observations indicated that oxidative damage to complex I proteins either did not result in increased ROS generation or that ROS were released into the mitochondrial matrix where they were eliminated by antioxidants. These data further support that in RWE-treated cells complex III was the major site of ROS released into the inner membrane space of mitochondria altering intracellular oxidative stress levels.

Induction of mitochondrial dysfunction by UQCRC2 deficiency in complex III

Oxidatively damaged mitochondrial proteins possess lower activity and they are subjected to enzymatic degradation (39). Because of the oxidative damage to UQCRC1 and UQCRC2 and the increased H_2O_2 release from complex III after RWE exposure, we further investigated the role of these proteins. To mimic their altered/decreased function, we down-regulated them at RNA level using ASO. The efficiency of ASO treatment was determined by quantitative RT-PCR. Results corrected by transfection frequency of cell cultures showed that ASO down-regulated their expression at RNA level by >80% (Fig. 5*A*). Due to varying percentage of

Table I. *Identification of oxidatively damaged protein*

Band No.[a]	Abbreviated Name	Protein Name	Gene Location	Molecular Mass (kDa)	*E* Value[b]	Access Swiss-Prot	Function	MRC	Mitochondrial Localization
1	NDUFS1	NADH dehydrogenase (ubiquinone) Fe-S	2q33-q34	75	7.3×10^{-12}	P28331	Electron transport	I	Inner membrane
3	NDUFS2	NADH dehydrogenase (ubiquinone) Fe-S	1q23	49	1.5×10^{-11}	O75306	Electron transport	I	Inner membrane
7	UQCRC1	Ubiquinol-cytochrome *c* reductase core 1	3p21.3	52	8.7×10^{-46}	P31930	Structural protein	III	Inner membrane associated
4, 8	UQCRC2	Ubiquinol-cytochrome *c* reductase core 2	16p12	48	9.2×10^{-45}	P22695	Structural protein	I, III	Inner membrane associated
5	GRP75[c]	75-kDa glucose-regulated protein	5q31.1	74	6.9×10^{-19}	P38646	Chaperone	III	Outer membrane
2, 6, 9, 11	HSP70[c]	Heat shock protein 70	5q31.1	74	3.5×10^{-29}	Q8N1C8	Chaperone	I, II, III, IV	Inner membrane associated
10, 12	HSP60[c]	Heat shock protein 60	2q33.1	61	3.7×10^{-28}	Q96RI4	Chaperone	II, IV	Matrix
13	CISY[c]	Citrate synthase	12q13.2-q13.3	52	6.9×10^{-19}	O75390	Krebs cycle	II	Matrix
14	VDAC1[c]	Voltage-dependent anion-selective channel protein 1	5q31	31	4.4×10^{-18}	P21796	Ion transport	II	Outer membrane

[a] Localization of bands is shown in Fig. 3*B*.
[b] Protein *E* value or expectation value assigned by the Mascot database is the number of matches with equal or better scores that are expected to occur by chance alone.
[c] Proteins co-migrated with MRCs in blue native PAGE (Fig. 3).

efficiently transfected cells (determined by Texas Red-labeled ASO), we used in situ microscopic analysis to assess changes in cellular ROS levels. Microscopic images indicated that only cells with red fluorescence (Texas Red) showed mitochondrial dysfunction as determined by increased DCF signal (green fluorescence) in UQCRC2 ASO-transfected cultures (Fig. 5*B*). The increased DCF fluorescence was seen at both 1 and 3 h after loading the cells with H_2DCF-DA, which is consistent with the sustained ROS generation shown in Fig. 1. In similar experiments UQCRC1 ASO-transfected cells showed no increased DCF fluorescence (data not shown). Taken together, these results suggested that down-regulation of UQCRC2 caused mitochondrial dysfunction.

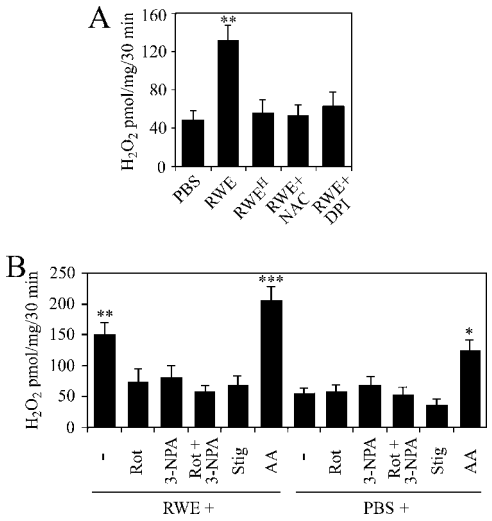

FIGURE 4. Mitochondria isolated from RWE-treated cells release higher amounts of H_2O_2 than do mitochondria isolated from mock-treated cells. *A*, Pretreatment of cells with antioxidant (NAC) as well as physical (heat treatment, RWE^H) or chemical (DPI) inactivation of pollen NADPH oxidases abolishes the ability of RWE to increase mitochondrial ROS generation. *B*, Identification of respiratory complex III as the major site of ROS production in mitochondria from RWE-treated cells. Administration of rotenone (Rot), 3-NPA, as well as stigmatellin (Stig) to mitochondria decreased RWE-induced mitochondrial ROS production, while addition of antimycin A (AA) enhanced RWE-induced mitochondrial ROS production. Data are presented as means ± SEM of three independent experiments. *, $p < 0.05$; **, $p < 0.01$; ***, $p < 0.001$ vs H_2O_2 release from mitochondria of mock-treated cells.

Preexisting mitochondrial dysfunction in the airways increases allergic inflammation and bronchial hyperresponsiveness

Next, we investigated whether a preexisting mitochondrial damage exacerbates allergic airway inflammation. Our plan was to model a natural situation in which individuals with mitochondrial dysfunction induced by environmental oxidants are exposed to pollen. In these experiments to induce mitochondrial dysfunction, the expression of UQCRC2 was down-regulated by ASO treatment in sensitized mice. The level of UQCRC2 in the airways was assessed immunohistochemically. We observed focal down-regulation of UQCRC2 (Fig. 6) in the bronchial epithelium; however, the expression of mitochondrially synthesized Cox IIb was not affected (Fig. 6). Mice expressing lower levels of UQCRC2 were intranasally challenged with RWE and the allergic inflammation was evaluated 72 h later (8). Differential cell counts from BALF showed a 4.4-fold increase in the number of eosinophils compared with those from mice challenged with RWE only (Fig. 7*A*). Down-regulation of UQCRC2 before RWE challenge also enhanced the accumulation of inflammatory cells in the peribronchial region of the airways (Fig. 7*B*). RWE challenge alone induced significant increase in inflammatory cell numbers in BALF compared with PBS challenge. Lower expression of UQCRC1 (Fig. 6) did not

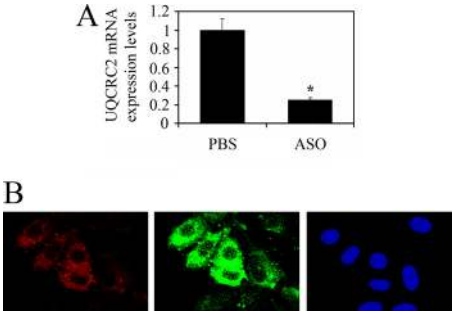

FIGURE 5. Down-regulation of UQCRC2 increases cellular ROS levels. *A*, ASO to UQCRC2 down-regulates its expression in LA-4 cells by >80% (see *Materials and Methods*). *B*, Increased ROS levels in cells efficiently transfected with ASO to UQCRC2. Cells were transfected with Texas Red-labeled ASO and various times thereafter cellular ROS levels were assessed by H_2DCF-DA using microscopic analysis. Only cells with red fluorescence (Texas Red) showed increased DCF signal (green fluorescence) in transfected cell cultures. *, $p < 0.05$ vs mock-treated cells.

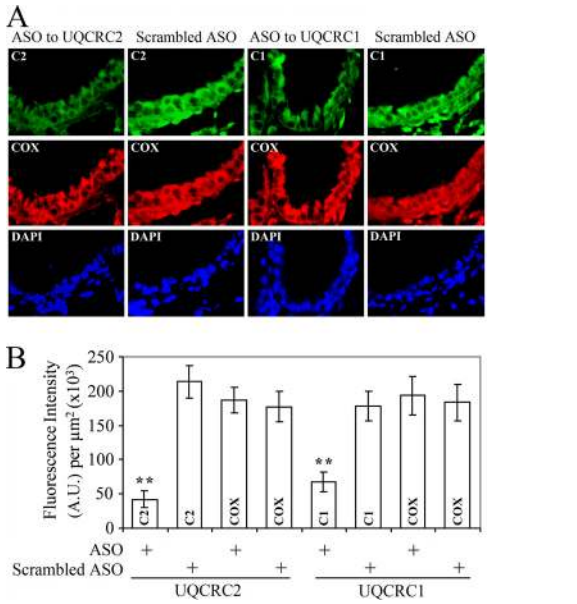

FIGURE 6. Inhibition of the expression of mitochondrial respiratory complex III core proteins in the lungs by local ASO treatment. *A*, ASO were administered intranasally to RWE-sensitized mice and expression of UQCRC1 and UQCRC2 was analyzed in lung sections by fluorescent microscopy. In the bronchial epithelium focal down-regulation of both UQCRC1 and UQCRC2 was observed (*left panel*); however, the expression of mitochondrially synthesized cytochrome *c* oxidase subunit IIb was not affected (*middle panel*). Scrambled ASO treatment did not modify the expression of either core proteins or Cox IIb (*left* and *middle panels*). *B*, Quantification of UQCRC1 and UQCRC2 expression in airway epithelial cells by measuring fluorescence signals in lung sections after staining with specific Abs (see *Materials and Methods*). Results are means ± SEM (n = 3–4 mice/group). A.U., arbitrary units; C1, UQCRC1; C2, UQCRC2; Cox, Cox IIb. **, $p < 0.01$ vs scrambled ASO treatment.

significantly increase the RWE-induced accumulation of eosinophils in the airways (Fig. 7). In controls, deficiency in levels of mitochondrial proteins alone did not increase number of eosinophils in BALF or recruit inflammatory cells to the peribronchial area (data not shown).

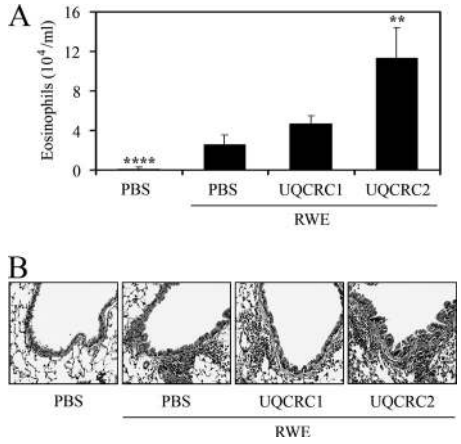

FIGURE 7. Preexisting mitochondrial dysfunction induced by UQCRC2 down-regulation increases RWE-induced accumulation of inflammatory cells in the airways. Antisense oligonucleotide treatment, specific for UQCRC2 but not for UQCRC1, increased the number of eosinophils in the bronchoalveolar lavage fluids (*A*) and enhanced accumulation of inflammatory cells in the peribronchial area (*B*) in RWE-challenged mice. **, $p < 0.01$ and ****, $p < 0.0001$ vs mock-treated, RWE-challenged mice.

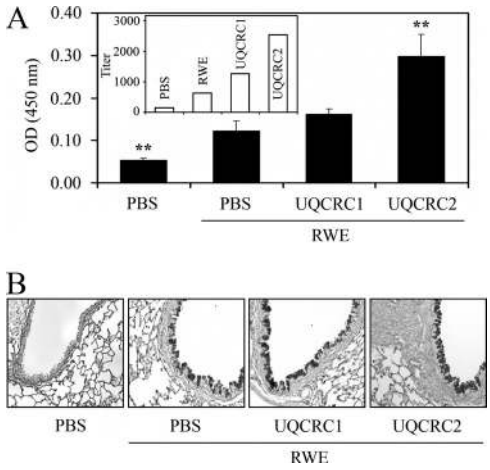

FIGURE 8. Mitochondrial dysfunction induced by UQCRC2 down-regulation enhances RWE-induced mucin production in the airways. Down-regulation of UQCRC2, but not UQCRC1, increased the levels of MUC5AC in the BALF (*A*) and increased the metaplasia of mucous cells in airway epithelium (*B*) of RWE-challenged mice. *Inset*, Endpoint titers of MUC5AC in the samples. **, $p < 0.01$ vs mock-treated, RWE-challenged mice.

Mucous cell proliferation and hypersecretion of airway mucin are important pathological features of asthma and allergic airway inflammation (40). The levels of MUC5AC, which is the most abundant mucin produced in the airway epithelial cells during allergic inflammation (41), were determined in the BALF by ELISA. The levels of the MUC5AC were 2.4-fold higher in the BALF of RWE-challenged mice deficient in UQCRC2 compared with those challenged with RWE only (Fig. 8*A*). As expected, decreased expression of UQCRC2 also enhanced the RWE-induced metaplasia of mucous cells in airway epithelium (Fig. 8*B*). Down-regulation of UQCRC1 before RWE challenge did not significantly increase either the MUC5AC levels in BALF or mucous cell metaplasia compared with mice challenged with RWE only (Fig. 8). Down-regulation of UQCRC2 or UQCRC1 alone did not induce mucous cell proliferation and metaplasia (data not shown).

As expected, airway hyperresponsiveness was increased (as reflected by Penh values) in all RWE-challenged groups of mice compared with those challenged with PBS (Fig. 9). However, mice expressing lower levels of UQCRC2, but not those of UQCRC1, showed a significant increase ($p < 0.01$) in airway hyperresponsiveness after RWE challenge compared with mice challenged with RWE only (Fig. 9). Penh values in mice deficient in UQCRC1 or UQCRC2 alone were similar to those in the saline-challenged control group (data not shown).

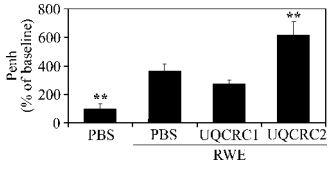

FIGURE 9. Preexisting mitochondrial dysfunction mediated by ASO to UQCRC2 increases RWE-induced airway hyperresponsiveness. Changes in pause of breathing (Penh) as an index of airway obstruction were measured by barometric whole-body plethysmography. **, $p < 0.01$ vs mock-treated, RWE-challenged mice.

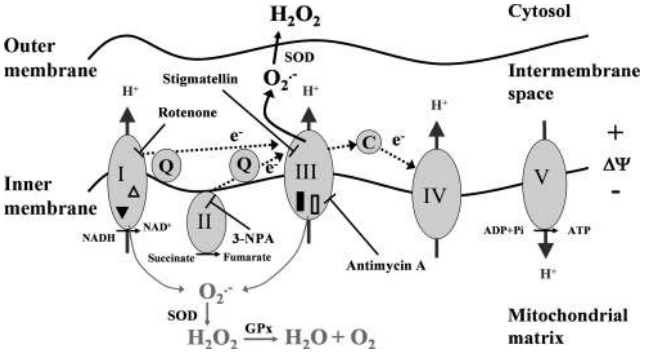

FIGURE 10. Schematic illustration of inner membrane complexes and localization of the oxidatively modified proteins in the mitochondria of RWE-treated cells. The mitochondrial respiratory chain consists of four multimeric complexes (complexes I–IV), coenzyme Q (Q), and cytochrome *c* (C). In RWE-treated cells ROS released to the cytosol are generated at the outer site of complex III. The primary generated reactive radical, superoxide anion ($O_2^{\cdot-}$), is converted into H_2O_2 by superoxide dismutases (SOD). Superoxide released into mitochondrial matrix at the inner sites of complexes I and III is converted to H_2O_2, which is then eliminated by catalase and glutathione peroxidases (GPx). The mitochondrial inner membrane is polarized (arrows) and mitochondrial membrane potential ($\Delta\Psi$) is maintained primarily by complex V. The symbols indicate the localization of NDUFS1 (▼) and NDUFS2 (△) in complex I, as well as UQCRC1 (■) and UQCRC2 (□) in complex III, being those proteins that are damaged by RWE-induced oxidative stress. The sites of action of respiratory chain inhibitors including rotenone, 3-NPA, stigmatellin, and antimycin A, which were used in this study, are also indicated.

Discussion

Allergic diseases are the leading cause of chronic diseases affecting >20% of the population worldwide. It has been shown that exposure to environmental oxidants causes exacerbation of allergic symptoms; however, the underlying mechanism is not fully understood. Prior studies demonstrated that environmental oxidants induce mitochondrial dysfunction in the lungs (5–7). Mitochondrial oxidative events are thought to be crucial in dendritic cell differentiation, Ag presentation, and in the generation of immune response that may lead to allergic inflammation (42). In an experimental model of asthma, marked mitochondrial ultrastructural changes and reduction in the expression of MRC proteins in airway epithelium were found to be associated with the local oxidative milieu created by recruited inflammatory cells (16). Here we show that preexisting mitochondrial dysfunction in airway epithelium exacerbates allergen-induced accumulation of eosinophils, mucin levels, and airway hyperresponsiveness.

To identify mitochondrial proteins sensitive to environmental oxidants, we treated cells with ragweed pollen (extract), which itself has intrinsic pro-oxidant activity (8). We have detected NDUFS1 and NDUFS2 from the catalytic core of complex I, as well as UQCRC1 and UQCRC2 structural proteins from complex III, as oxidatively damaged MRC proteins in these cells (Fig. 10). Mitochondria isolated from RWE-treated cells showed increased release of H_2O_2, suggesting that oxidative damage to respiratory chain proteins is directly related to mitochondrial dysfunction. To identify the site of ROS generation in oxidatively damaged mitochondria, we used inhibitors of respiratory chain complexes. Our results show that the combined use of rotenone, which inhibits the electron flow at complex I near the binding site for ubiquinol, the electron acceptor for complex I (43), and 3-NPA, which irreversibly binds to succinate dehydrogenase in complex II (44), blocked H_2O_2 generation in mitochondria from RWE-treated cells, indicating that the electron transport chain, but not α-ketoglutarate dehydrogenase in the Krebs cycle (45), is the major source of ROS. Stigmatellin, which blocks complex III at the Qo site, at submicromolar concentrations (38) also abolished mitochondrial ROS generation. In contrast, antimycin A, which binds to the matrix side of complex III and inhibits the Qi site of cytochrome *c* oxidoreductase in the cytochrome *b* subunit (21), further increased the RWE treatment-induced mitochondrial ROS production. These studies together suggest that complex III is the main site for ROS generation in mitochondria of RWE-exposed cells, and thus we focused on core I and II proteins in respiratory complex III.

Both UQCRC1 and UQCRC2 are localized to the matrix side of complex III in proximity to the predicted site of ROS generation at Qi center. These proteins provide structural stability to complex III and they have mitochondrial processing peptidase activity (46). UQCRC1 and UQCRC2 have been identified among the oxidatively damaged proteins in mitochondria from kidney (47), skeletal muscle (48), and heart (48) in aging mice. Moreover, UQCRC2 was found to be involved in the natural senescence of mouse brain (49). Oxidative stress that occurs in response to pathogens also induces oxidative modification (e.g., carbonylation) to these core proteins (50). Taken together, our results suggest that core proteins in complex III are the primary acceptors of reactive radicals, and oxidative damage-induced alterations in their structure and/or function lead to increased mitochondrial ROS production.

Increased protein degradation results in subphysiological levels of functional proteins (accumulation of oxidatively modified and dysfunctional proteins) (39, 51, 52). To mimic the transient decrease in levels and/or functions of the oxidatively damaged UQCRC1 and UQCRC2, we down-regulated their expression by antisense oligonucleotides before RWE challenge. We found that deficiency of UQCRC2, but not UQCRC1, enhanced cellular ROS levels. Although UQCRC1 and UQCRC2 share many characteristics, it seems that they have different roles in the maintenance of ubiquinol-cytochrome *c* reductase activity of complex III. Partial processing of UQCRC2 is shown to be associated with impairment of proton pumping, suggesting that UQCRC2 has an important role in the maintenance of inner membrane potential and thereby in mitochondrial ROS generation (53). UQCRC2 is required for the assembly of complex III, possessing two ubiquinone-reactive centers through which electrons are forwarded to cytochrome *c* oxidase. The Qo center, where ubiquinol is oxidized by redox active centers cytochrome *c*1 and the "Rieske" (2Fe-2S) protein, is oriented toward the intermembrane space, while the Qi center, where ubiquinone is reduced by the redox center cytochrome *b*, is facing the matrix (54). Antimycin A inhibits the Qi center, thus increasing H_2O_2 release from mitochondria. Analogously, RWE-mediated oxidative damage to UQCRC2 might perturb electron flow at the Qi center, thus directing electrons to the intermembrane space to reduce molecular oxygen to form $O_2^{\cdot-}$ and consequently inducing elevated mitochondrial ROS production. In addition to mitochondrial complex subunit proteins, several accessory proteins were oxidatively damaged in the mitochondria of RWE-treated cells. Although the roles of these proteins are significant in maintaining mitochondrial integrity and function, they are not directly involved in mitochondrial ROS generation.

We demonstrated that exposure to RWE induced sustained ROS generation in A549 cells, while in the isogenic *ρ0* cells only transient oxidative burst was observed. These results strongly suggest that mtDNA-encoded proteins are implicated in the prolonged ROS generation. However, we found that genomic DNA-encoded mitochondrial proteins were damaged in RWE-treated cells. The lack of mtDNA-encoded damaged proteins may be due to the protective effects of nuclear DNA-derived accessory and structural

proteins or their oxidative damage cannot be detected by the applied methods. Out of nearly a thousand proteins in the mitochondria that are required for their function, only 13 are encoded by mtDNA (55). Although we cannot exclude damage to mitochondrial DNA-encoded proteins, our results suggest that nuclear DNA-encoded, oxidatively modified mitochondrial proteins are associated with mitochondrial dysfunction in RWE-treated cells.

Mitochondrial dysfunction and ultrastructural changes (loss of cristae and swelling) have been observed as consequences of airway inflammation in an experimental allergic asthma model (16). Epidemiological studies have revealed that there is a link between maternal history of atopy and susceptibility to atopic disorders of the descendant (18, 56). Furthermore, a mitochondrial haplogroup has been shown to be associated with increased serum IgE levels in asthmatics (20). Since mitochondria are inherited through the maternal line, it raises the possibility that sequence variation in the mitochondrial genome is related to the pathogenesis of asthma and atopy.

Our data indicate that nuclear DNA-encoded mitochondrial proteins are also involved in the exacerbation of RWE-induced allergic inflammation. Indeed, an increase in the intensity of allergic responses in mice was related to the chromosome 16-encoded UQCRC2. UQCRC2 has not been linked to airway inflammation yet, while it is implicated in a sex-dependent response to stress in overweight women (57). It is noteworthy that obesity is a major risk factor for asthma (58), and this association is most consistent in women (59). UQCRC2 is important in maintenance of mitochondrial functional integrity, and thus its preferential carbonylation may be associated with mitochondria-driven cellular changes leading to altered lung function or airway hyperresponsiveness phenotype, which is independent from mitochondrial haplogroups (60). Since the polymorphism of UQCRC2 has already been reported (National Center for Biotechnology Information, Single Nucleotide Polymorphism database, gene ID no. 7385), future studies are needed to investigate its possible association with atopy in humans. Our data showing that preexisting mitochondrial dysfunction enhances allergic inflammation are in line with previous observations. Exposure to ozone or particulate matter air pollution, both of which induce mitochondrial damage (5, 6), before allergen challenge significantly enhanced the allergic responses (61, 62). Furthermore, when pollen was administered daily to ragweed-sensitized patients, smaller doses were required on each succeeding day to cause the same or greater degree of allergic symptoms (11). Repeated challenges of the nasal membrane with pollen also increased the symptoms to another allergen and to nonallergic stimuli (11). Another human study showed that rechallenge with pollen after 3 days, but not 1 or 4 wk later, resulted in extensive allergic clinical symptoms and inflammatory cell infiltration (12). Taking these and our observations into consideration, oxidative damage-induced mitochondrial dysfunction may be involved in the "priming" phenomenon; however, this idea needs further investigation.

In conclusion, we provide evidence for the first time that oxidative damage to specific proteins in the mitochondria prior the Ag exposure intensifies airway eosinophilia, increases mucin production, and enhances bronchial hyperresponsiveness. Our data also imply that prevention or reduction of oxidative mitochondrial damage in the airways may have a beneficial role in therapy of these diseases.

Disclosures

The authors have no financial conflicts of interest.

References

1. Holgate, S. T. 1999. Genetic and environmental interaction in allergy and asthma. *J. Allergy Clin. Immunol.* 104: 1139–1146.
2. Bowler, R. P. 2004. Oxidative stress in the pathogenesis of asthma. *Curr. Allergy Asthma Rep.* 4: 116–122.
3. Riedl, M. A., and A. E. Nel. 2008. Importance of oxidative stress in the pathogenesis and treatment of asthma. *Curr. Opin. Allergy Clin. Immunol.* 8: 49–56.
4. Ott, M., V. Gogvadze, S. Orrenius, and B. Zhivotovsky. 2007. Mitochondria, oxidative stress and cell death. *Apoptosis* 12: 913–922.
5. Servais, S., A. Boussouar, A. Molnar, T. Douki, J. M. Pequignot, and R. Favier. 2005. Age-related sensitivity to lung oxidative stress during ozone exposure. *Free Radical Res.* 39: 305–316.
6. Li, N., C. Sioutas, A. Cho, D. Schmitz, C. Misra, J. Sempf, M. Wang, T. Oberley, J. Froines, and A. Nel. 2003. Ultrafine particulate pollutants induce oxidative stress and mitochondrial damage. *Environ. Health Perspect.* 111: 455–460.
7. Fahn, H. J., L. S. Wang, S. H. Kao, S. C. Chang, M. H. Huang, and Y. H. Wei. 1998. Smoking-associated mitochondrial DNA mutations and lipid peroxidation in human lung tissues. *Am. J. Respir. Cell Mol. Biol.* 19: 901–909.
8. Boldogh, I., A. Bacsi, B. K. Choudhury, N. Dharajiya, R. Alam, T. K. Hazra, S. Mitra, R. M. Goldblum, and S. Sur. 2005. ROS generated by pollen NADPH oxidase provide a signal that augments antigen-induced allergic airway inflammation. *J. Clin. Invest.* 115: 2169–2179.
9. Bacsi, A., B. K. Choudhury, N. Dharajiya, S. Sur, and I. Boldogh. 2006. Subpollen particles: carriers of allergenic proteins and oxidases. *J. Allergy Clin. Immunol.* 118: 844–850.
10. Dharajiya, N., B. K. Choudhury, A. Bacsi, I. Boldogh, R. Alam, and S. Sur. 2007. Inhibiting pollen reduced nicotinamide adenine dinucleotide phosphate oxidase-induced signal by intrapulmonary administration of antioxidants blocks allergic airway inflammation. *J. Allergy Clin. Immunol.* 119: 646–653.
11. Connell, J. T. 1969. Quantitative intranasal pollen challenges, 3: The priming effect in allergic rhinitis. *J. Allergy* 43: 33–44.
12. Ciprandi, G., V. Ricca, M. Landi, G. Passalacqua, M. Bagnasco, and G. W. Canonica. 1998. Allergen-specific nasal challenge: response kinetics of clinical and inflammatory events to rechallenge. *Int. Arch. Allergy Immunol.* 115: 157–161.
13. Batinic-Haberle, I., L. Benov, I. Spasojevic, and I. Fridovich. 1998. The ortho effect makes manganese(III) meso-tetrakis(*N*-methylpyridinium-2-yl)porphyrin a powerful and potentially useful superoxide dismutase mimic. *J. Biol. Chem.* 273: 24521–24528.
14. Spasojevic, I., Y. Chen, T. J. Noel, Y. Yu, M. P. Cole, L. Zhang, Y. Zhao, D. K. St Clair, and I. Batinic-Haberle. 2007. Mn porphyrin-based superoxide dismutase (SOD) mimic, MnIIITE-2-PyP5$^+$, targets mouse heart mitochondria. *Free Radical Biol. Med.* 42: 1193–1200.
15. Chang, L. Y., and J. D. Crapo. 2002. Inhibition of airway inflammation and hyperreactivity by an antioxidant mimetic. *Free Radical Biol. Med.* 33: 379–386.
16. Mabalirajan, U., A. K. Dinda, S. Kumar, R. Roshan, P. Gupta, S. K. Sharma, and B. Ghosh. 2008. Mitochondrial structural changes and dysfunction are associated with experimental allergic asthma. *J. Immunol.* 181: 3540–3548.
17. Giles, R. E., H. Blanc, H. M. Cann, and D. C. Wallace. 1980. Maternal inheritance of human mitochondrial DNA. *Proc. Natl. Acad. Sci. USA* 77: 6715–6719.
18. Litonjua, A. A., V. J. Carey, H. A. Burge, S. T. Weiss, and D. R. Gold. 1998. Parental history and the risk for childhood asthma: does mother confer more risk than father? *Am. J. Respir. Crit. Care Med.* 158: 176–181.
19. Kurukulaaratchy, R. J., S. Matthews, and S. H. Arshad. 2006. Relationship between childhood atopy and wheeze: what mediates wheezing in atopic phenotypes? *Ann. Allergy Asthma Immunol.* 97: 84–91.
20. Raby, B. A., B. Klanderman, A. Murphy, S. Mazza, C. A. Camargo, Jr., E. K. Silverman, and S. T. Weiss. 2007. A common mitochondrial haplogroup is associated with elevated total serum IgE levels. *J. Allergy Clin. Immunol.* 120: 351–358.
21. Bacsi, A., M. Woodberry, W. Widger, J. Papaconstantinou, S. Mitra, J. W. Peterson, and I. Boldogh. 2006. Localization of superoxide anion production to mitochondrial electron transport chain in 3-NPA-treated cells. *Mitochondrion* 6: 235–244.
22. King, M. P., and G. Attardi. 1996. Isolation of human cell lines lacking mitochondrial DNA. *Methods Enzymol.* 264: 304–313.
23. Dobson, A. W., V. Grishko, S. P. LeDoux, M. R. Kelley, G. L. Wilson, and M. N. Gillespie. 2002. Enhanced mtDNA repair capacity protects pulmonary artery endothelial cells from oxidant-mediated death. *Am. J. Physiol.* 283: L205–L210.
24. Aguilera-Aguirre, L., J. C. Gonzalez-Hernandez, V. Perez-Vazquez, J. Ramirez, M. Clemente-Guerrero, R. Villalobos-Molina, and A. Saavedra-Molina. 2002. Role of intramitochondrial nitric oxide in rat heart and kidney during hypertension. *Mitochondrion* 1: 413–423.
25. Saavedra-Molina, A., S. Uribe, and T. M. Devlin. 1990. Control of mitochondrial matrix calcium: studies using fluo-3 as a fluorescent calcium indicator. *Biochem. Biophys. Res. Commun.* 167: 148–153.
26. Schagger, H. 2001. Blue-native gels to isolate protein complexes from mitochondria. *Methods Cell Biol.* 65: 231–244.
27. Van Coster, R., J. Smet, E. George, L. De Meirleir, S. Seneca, J. Van Hove, G. Sebire, H. Verhelst, J. De Bleecker, B. Van Vlem, et al. 2001. Blue native polyacrylamide gel electrophoresis: a powerful tool in diagnosis of oxidative phosphorylation defects. *Pediatr. Res.* 50: 658–665.
28. Forbus, J., H. Spratt, J. Wiktorowicz, Z. Wu, I. Boldogh, L. Denner, A. Kurosky, R. C. Brasier, B. Luxon, and A. R. Brasier. 2006. Functional analysis of the nuclear proteome of human A549 alveolar epithelial cells by HPLC-high resolution 2-D gel electrophoresis. *Proteomics* 6: 2656–2672.

29. Trinidad, J. C., C. G. Specht, A. Thalhammer, R. Schoepfer, and A. L. Burlingame. 2006. Comprehensive identification of phosphorylation sites in postsynaptic density preparations. *Mol. Cell. Proteomics* 5: 914–922.
30. Estabrook, R. W. 1967. Mitochondrial respiratory control and the polarographic measurement of ADP:O ratios. In *Methods in Enzymology.* R. W. Estabrook and M. E. Pullman, eds. Academic, New York, pp. 41–47.
31. Boldogh, I., L. Aguilera-Aguirre, A. Bacsi, B. K. Choudhury, A. Saavedra-Molina, and M. Kruzel. 2008. Colostrinin decreases hypersensitivity and allergic responses to common allergens. *Int. Arch. Allergy Immunol.* 146: 298–306.
32. Adler, A., G. Cieslewicz, and C. G. Irvin. 2004. Unrestrained plethysmography is an unreliable measure of airway responsiveness in BALB/c and C57BL/6 mice. *J. Appl. Physiol.* 97: 286–292.
33. Sur, S., J. S. Wild, B. K. Choudhury, N. Sur, R. Alam, and D. M. Klinman. 1999. Long term prevention of allergic lung inflammation in a mouse model of asthma by CpG oligodeoxynucleotides. *J. Immunol.* 162: 6284–6293.
34. Bacsi, A., N. Dharajiya, B. K. Choudhury, S. Sur, and I. Boldogh. 2005. Effect of pollen-mediated oxidative stress on immediate hypersensitivity reactions and late-phase inflammation in allergic conjunctivitis. *J. Allergy Clin. Immunol.* 116: 836–843.
35. Van Gestelen, P., H. Asard, and R. J. Caubergs. 1997. Solubilization and separation of a plant plasma membrane NADPH-O_2-synthase from other NAD(P)H oxidoreductases. *Plant Physiol.* 115: 543–550.
36. Loschen, G., A. Azzi, C. Richter, and L. Flohe. 1974. Superoxide radicals as precursors of mitochondrial hydrogen peroxide. *FEBS Lett.* 42: 68–72.
37. Xia, T., M. Kovochich, and A. E. Nel. 2007. Impairment of mitochondrial function by particulate matter (PM) and their toxic components: implications for PM-induced cardiovascular and lung disease. *Front. Biosci.* 12: 1238–1246.
38. Degli Esposti, M., A. Ghelli, M. Crimi, E. Estornell, R. Fato, and G. Lenaz. 1993. Complex I and complex III of mitochondria have common inhibitors acting as ubiquinone antagonists. *Biochem. Biophys. Res. Commun.* 190: 1090–1096.
39. Bulteau, A. L., L. I. Szweda, and B. Friguet. 2006. Mitochondrial protein oxidation and degradation in response to oxidative stress and aging. *Exp. Gerontol.* 41: 653–657.
40. Tanizaki, Y., H. Kitani, M. Okazaki, T. Mifune, F. Mitsunobu, and I. Kimura. 1993. Mucus hypersecretion and eosinophils in bronchoalveolar lavage fluid in adult patients with bronchial asthma. *J. Asthma* 30: 257–262.
41. Thornton, D. J., I. Carlstedt, M. Howard, P. L. Devine, M. R. Price, and J. K. Sheehan. 1996. Respiratory mucins: identification of core proteins and glycoforms. *Biochem. J.* 316: 967–975.
42. Del Prete, A., P. Zaccagnino, M. Di Paola, M. Saltarella, C. Oliveros Celis, B. Nico, G. Santoro, and M. Lorusso. 2008. Role of mitochondria and reactive oxygen species in dendritic cell differentiation and functions. *Free Radical Biol. Med.* 44: 1443–1451.
43. Chen, Q., E. J. Vazquez, S. Moghaddas, C. L. Hoppel, and E. J. Lesnefsky. 2003. Production of reactive oxygen species by mitochondria: central role of complex III. *J. Biol. Chem.* 278: 36027–36031.
44. Coles, C. J., D. E. Edmondson, and T. P. Singer. 1979. Inactivation of succinate dehydrogenase by 3-nitropropionate. *J. Biol. Chem.* 254: 5161–5167.
45. Adam-Vizi, V. 2005. Production of reactive oxygen species in brain mitochondria: contribution by electron transport chain and non-electron transport chain sources. *Antioxid. Redox Signal.* 7: 1140–1149.
46. Deng, K., S. K. Shenoy, S. C. Tso, L. Yu, and C. A. Yu. 2001. Reconstitution of mitochondrial processing peptidase from the core proteins (subunits I and II) of bovine heart mitochondrial cytochrome bc1 complex. *J. Biol. Chem.* 276: 6499–6505.
47. Choksi, K. B., J. E. Nuss, W. H. Boylston, J. P. Rabek, and J. Papaconstantinou. 2007. Age-related increases in oxidatively damaged proteins of mouse kidney mitochondrial electron transport chain complexes. *Free Radical Biol. Med.* 43: 1423–1438.
48. Choksi, K. B., J. E. Nuss, J. H. Deford, and J. Papaconstantinou. 2008. Age-related alterations in oxidatively damaged proteins of mouse skeletal muscle mitochondrial electron transport chain complexes. *Free Radical Biol. Med.* 45: 826–838.
49. Lad, S. P., G. Yang, D. A. Scott, T. H. Chao, S. Correia Jda, J. C. de la Torre, and E. Li. 2008. Identification of MAVS splicing variants that interfere with RIGI/MAVS pathway signaling. *Mol. Immunol.* 45: 2277–2287.
50. Wen, J. J., and N. Garg. 2004. Oxidative modification of mitochondrial respiratory complexes in response to the stress of *Trypanosoma cruzi* infection. *Free Radical Biol Med.* 37: 2072–2081.
51. Shringarpure, R., T. Grune, and K. J. Davies. 2001. Protein oxidation and 20S proteasome-dependent proteolysis in mammalian cells. *Cell. Mol. Life Sci.* 58: 1442–1450.
52. Jung, T., and T. Grune. 2008. The proteasome and its role in the degradation of oxidized proteins. *IUBMB Life* 60: 743–752.
53. Cocco, T., M. Di Paola, S. Papa, and M. Lorusso. 1998. Chemical modification of the bovine mitochondrial bc1 complex reveals critical acidic residues involved in the proton pumping activity. *Biochemistry* 37: 2037–2043.
54. Iwata, S., J. W. Lee, K. Okada, J. K. Lee, M. Iwata, B. Rasmussen, T. A. Link, S. Ramaswamy, and B. K. Jap. 1998. Complete structure of the 11-subunit bovine mitochondrial cytochrome bc1 complex. *Science* 281: 64–71.
55. Scarpulla, R. C. 2008. Transcriptional paradigms in mammalian mitochondrial biogenesis and function. *Physiol. Rev.* 88: 611–638.
56. Soto-Quiros, M. E., E. K. Silverman, L. A. Hanson, S. T. Weiss, and J. C. Celedon. 2002. Maternal history, sensitization to allergens, and current wheezing, rhinitis, and eczema among children in Costa Rica. *Pediatr. Pulmonol.* 33: 237–243.
57. Hittel, D. S., W. E. Kraus, C. J. Tanner, J. A. Houmard, and E. P. Hoffman. 2005. Exercise training increases electron and substrate shuttling proteins in muscle of overweight men and women with the metabolic syndrome. *J. Appl. Physiol.* 98: 168–179.
58. Romieu, I., V. Avenel, B. Leynaert, F. Kauffmann, and F. Clavel-Chapelon. 2003. Body mass index, change in body silhouette, and risk of asthma in the E3N cohort study. *Am. J. Epidemiol.* 158: 165–174.
59. Chen, Y., R. Dales, M. Tang, and D. Krewski. 2002. Obesity may increase the incidence of asthma in women but not in men: longitudinal observations from the Canadian National Population Health Surveys. *Am. J. Epidemiol.* 155: 191–197.
60. Raby, B. A., K. Van Steen, J. C. Celedon, A. A. Litonjua, C. Lange, and S. T. Weiss. 2005. Paternal history of asthma and airway responsiveness in children with asthma. *Am. J. Respir. Crit. Care Med.* 172: 552–558.
61. Molfino, N. A., S. C. Wright, I. Katz, S. Tarlo, F. Silverman, P. A. McClean, J. P. Szalai, M. Raizenne, A. S. Slutsky, and N. Zamel. 1991. Effect of low concentrations of ozone on inhaled allergen responses in asthmatic subjects. *Lancet* 338: 199–203.
62. Hauser, R., T. M. Rice, G. G. Krishna Murthy, M. P. Wand, D. Lewis, T. Bledsoe, and J. Paulauskis. 2003. The upper airway response to pollen is enhanced by exposure to combustion particulates: a pilot human experimental challenge study. *Environ. Health Perspect.* 111: 472–477.